Feedforward Effect On The Transient Response During Low Voltage Ride Through

Raul De La Fuente Pinto*, Philipp Thies, Mohammad Abusara

[1]Renewable Energy department University of Exeter, Penryn, UK
** rd477@exeter.ac.uk*

Keywords: Control methods, Feedforward, grid, LVRT, Grid-connected, current overshoot

Abstract

Suitable control methods and strategies applied in Power Electronic converters are vital to interconnecting renewable energy sources within a microgrid and the utility grid. Grid codes and international standards are introducing new specifications according to the rapid changes the electric power systems are experiencing in the last decades. Therefore, developing, testing and upgrading the control methods to fulfil those new standards is essential. This paper focuses on the Low Voltage Ride Through (LVRT) capability applied in an industrial inverter connected to the grid through an LCL filter with a maximum admissible inverter-side current of 1.23 p.u. The main challenge is that the protective circuit shuts the inverter down once maximum current is exceeded (as a result of a sudden drop in grid voltage) and disconnects from the grid; hence making it not compliant with the standards. This paper investigates the effect of the Feedforward voltage loop on the inverter side peak current and suggests solutions to limit the current based on modifying the feedforward structure and tuning the controller parameters. Simulation results show a reduction in the inverter side current from 1.89 pu to 1.09.

1 Introduction

1.1 *Introduction*

Due to the fast energy transition from fossil fuels to renewable energy resources, the electric power system loses its mechanical inertia because old coal power plants are closing. This is especially the case in many emerging economies, such as South Africa [1]. Therefore the utility networks become fragile and increasingly vulnerable in front of perturbances that can make them unstable, ending in undesirable situations such as blackouts or service interruptions. As a result, the electric network becomes weak and unreliable. This research paper is part of a project to interconnect a solar farm to the utility grid, when available, in Dornkoop village at 100 miles northeast of Johannesburg, South Africa, where the grid presents the same characteristics.

For this reason, the grid codes impose the Low Voltage Ride Through (LVRT) for all Distributed Generators, including solar energy. LVRT is the capability of a power plant to remain connected to the Electric Power network, in front of a voltage drop, with the mission of contributing to clear the fault injecting reactive current during a short period, typically in the order of 150 ms. Thus, the Power Electronic device must remain connected above the voltage limits and only disconnect when the fault is longer than those boundaries. The specific limits differ for each country.

Fig. 1. Shows the limits applied to power plants with non-synchronous machines and with power equal to or over 100 kW up to 1MW [2]. According to the South African grid code, only Power plants with a rated power of 1MW or higher shall inject reactive current.

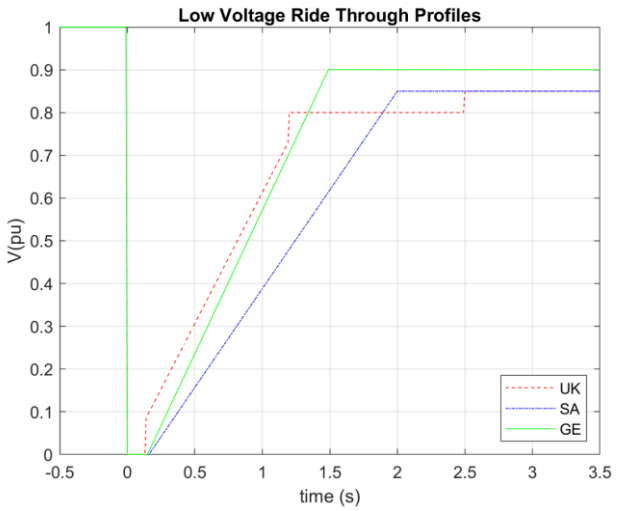

Fig. 1. Comparison of LVRT limits between UK, South African, and German grid codes [2,3,4]

A voltage drop occurs typically for three reasons: short circuits, overloads or connection of inductive loads into the grid. The common characteristic of these three events is that the current increases exponentially, posing a challenge for grid-connected inverters. They have to remain connected during the voltage fault and support the current spikes even though the peaks surpass the maximum limits of the devices. Some of the solutions proposed in the literature are discussed below.

It is common practice to limit the current setpoint to avoid undesirable peaks, as in the comparison made by Green and Bottelli [5]. Further studies to enhance the limitation techniques considering the THD are presented by [6].

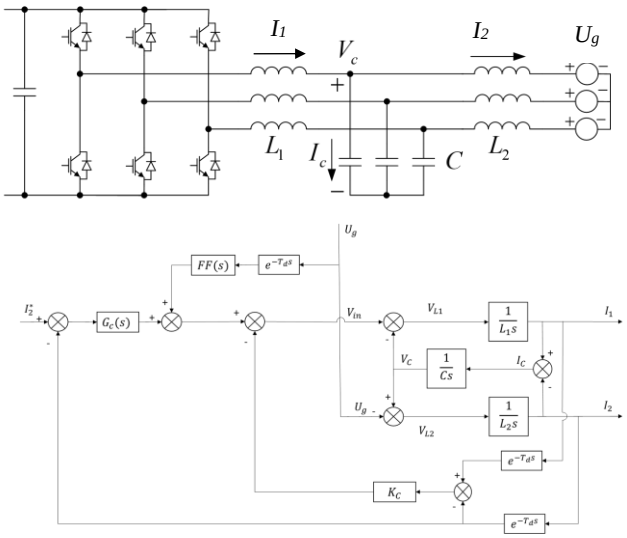

Fig. 2. DC/AC converter and controller block diagram with the Volage Feedforward in the abc reference frame

However, part of the algorithm has to monitor the current constantly to compare it with a maximum value to apply the limitation. Therefore there is a time delay between the fault detection and the control action. On the other hand, reactive current injection techniques fulfil the grid codes without exceeding the maximum current allowed by the IGBT [7]. However, in the study, the grid voltage never drops below 50%.

There are currently no studies conducted considering the effect of the grid voltage feedforward on the current peak during LVRT. Although the voltage Feedforward loop has been successfully implemented to reject the grid's harmonics and reduce steady state errors [8], its effect on limiting peak current during LVRT has not been investigated.

This paper aims to investigate the effect of a sudden drop in the grid voltage on the increase of the inverter current. It proposes solutions to limit the pake of the current by implementing a feedforward control loop of the grid voltage and tuning of the control parameters. Limiting the inverter current is important to make sure that the high current protective circuits are not triggered and the inverter continues to operate safely during LVRT.

1.2 System description

1.2.1 DC/AC converter and controller system

The power converter subject to study is a three-phase industrial inverter rated at 200A rms connected to the grid at 230V rms 50Hz, able to supply loads with a Power factor of 0.72. Fig. 2 shows the schematic of the converter and a simplified block diagram in the continuous-time domain, including the computational time delay and showing two outputs. Table 1 shows the values of the system parameters.

From Fig. 2, FF(S) is the theoretical Feedforward given by [8]:

$$FF(s) = L_1 C s^2 + K_c C s + 1 \quad (1)$$

$G_c(s)$ is a PI controller wich expression is:

$$G(S) = K_p + \frac{K_i}{s} \quad (2)$$

Table 1 System parameters

Inverter parameters	
Voltage (V)	230
Current (A)	200
Power (kW)	100
L_1 (µH)	250
L_2 (µH)	50
C (µF)	200
Controller parameters	
Kp	2
Ki	100
Kc	2
Td (µs)	25

1.2.2 LCL filter

Available research has considered the design of LCL filter to suppress current overshoots when the grid voltage drops [10]. However, it does not apply to inverters already designed because resizing the components implies more volume and cost. However, studying the filter design shows that when the fault is produced, the physical components of the filter take control during one or two switching periods to allow the energy stored in the inductor and capacitor to be released, causing the current to surge.

A single-phase LCL filter is represented in Fig. 3. To understand the current variation during voltage sags in the grid, the following dynamic equations are derived:

$$\frac{di_1}{dt} = \frac{-u_c}{L_1} + \frac{u_{in}}{L_1} \quad (3)$$

$$\frac{di_2}{dt} = \frac{u_c}{L_2} - \frac{u_{out}}{L_2} \quad (4)$$

$$\frac{du_c}{dt} = \frac{i_1}{C} - \frac{i_2}{C} \quad (5)$$

We can see that the variation in both currents is inversely proportional to the inductor value. Therefore, these values are fixed by design. The only other factor is the difference voltage between the input and the capacitor for the inverter side

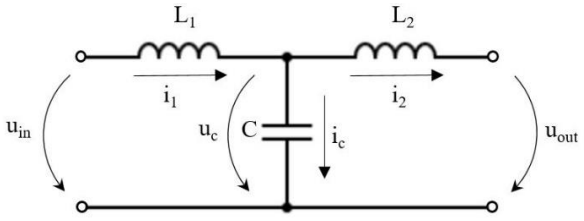

Fig. 3. LCL filter schematic

inductor and from the capacitor and the grid voltage for the grid side inductor.

The input voltage is coming from the control action PWM. Hence we can assume that designing a controller can equal the voltages, and the current peak can be reduced.

2 System analysis

In order to simulate a symmetrical shortcircuit between the three phases and ground, an AC variable voltage sources have been simulated by a ramp with a change rate from V_{max} to 0 V in 200 µs.The fault time has been selected at 85 ms since the voltage is at its maximum value, worse case, and the output had enough time to reach the steady-state without Feedforward.

2.1 System transfer functions

The output current (grid side current) is represented by transfer functions that relate the current itself with the current setpoint and the grid voltage which is represented as a disturbance in the block diagram of Fig. 2. In this study, we studied the inverter side current as an output, because it is the system output we want to reduce its peak in order prevent the high current protection circuit from being activated. Then the system, can be described with four Transfer functions to relate the two inputs with the two outputs.

The theoretical FeedForward (1) has been considered and it is noted that it cancels the grid voltage disturbance over the output current as shown in (7) but influences the first inductor current with a derivative term as shown in (6).

$$i_1 = \frac{K_p C L_2 s^3 + K_i C L_2 s^2 + K_p s + K_i}{C L_1 L_2 s^4 + C K_c L_2 s^3 + (L_1 + L_2) s^2 + K_p s + K_i} \cdot i_{sp} + K_c C s \cdot u_{out} \quad (6)$$

$$i_2 = \frac{K_p s + K_i}{C L_1 L_2 s^4 + C K_c L_2 s^3 + (L_1 + L_2) s^2 + K_p s + K_i} \cdot i_{sp} + 0 \cdot u_{out} \quad (7)$$

2.2 High pass filter as a differentiator

The transfer function (1) contains two pure derivatives terms. However, it is well known that the practical implementation of the pure derivatives become a problem because they can amplify undesirable electrical noises, so unlike the theory, the whole system can become unstable[11].

However, the derivative can be approximated as a high pass filter such as [11]:

$$HPF(s) = \frac{\omega_c s}{s + \omega_c} \quad (8)$$

where ω_c, it is the cut-off frequency.

The final form of the FF transfer function is shown below

$$FF(s) = 1 + K_c C \frac{\omega_c s}{s + \omega_c} \quad (9)$$

To obtain the same response as a pure derivative, 90º phase shift, and the correct gain, the filter's cut-off frequency has been chosen to be ten times the resonance frequency (10) of the filter since the oscillations observed during the transitory response have the same order of magnitude.

$$\omega_c = 10x\sqrt{\frac{L_1 + L_2}{L_1 x L_2 x C}} \approx 1x10^5\ rad/s \quad (10)$$

We choose the Tustin approximation to transform the filter from continuous to the discrete domain [12]. The filters transfer functions are expressed in Table 2. With this cut-off frequency, the output of the filter is 90 º shifted and the gain of 80 dB.

Table 2. High Pass Filter transfer functions

Domain	Transfer functions
Continous domain	$\frac{1.095\ \text{x}10^5 s}{s + 1.095\ \text{x}10^5}$
Discrete domain	$\frac{2.477 \cdot 10^4 z - 2.477 \cdot 10^4}{z + 0.5478}$

2.3 Closed-loop transfer function step response

Alternatively, arranging equation (9), we can derive a similar form of the inverse of a lead compensator as follow:

$$FF(S) = (1 + K_c C \omega_c) \frac{s + \frac{1}{(1 + K_c C \omega_c) T_C}}{s + \frac{1}{T_C}} \quad (11)$$

From Fig. 2, we can obtain the diagram in Fig4. Applying block diagram reduction methods [13], and considering the time delay as a second-order Padé approximation [11], we

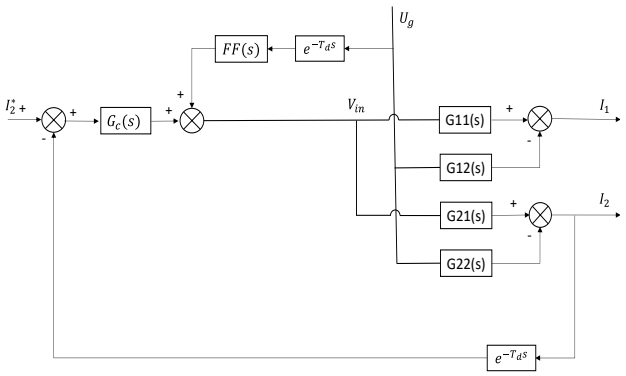

Fig. 4. Reduced block diagram

obtain G11(s), G12(s), G21(s), G22(s), which are transfer functions including the current capacitor inner loop.

Applying the superposition method, we can derive the close loop transfer function (12) and (13), which relate the inverter side inductor current (I_1) with the perturbance (U_g), and the current demand (I_2^*) respectively. Different analysis has been performed to determine the ω_c to minimise the overshoot.

$$\frac{I_1}{U_g} = \frac{G11(s)FF(s)TD(s)+G11G_c(s)G22(s)-G12(s)-G12(s)G21(s)G_c(s)}{1+G21(s)G_c(s)} \quad (12)$$

$$\frac{I_1}{I_2^*} = \frac{G11(s)G_c(s)+G11G_c^2(s)G21(s)}{1+G21(s)G_c(s)TD(s)} \quad (13)$$

From the poles and zeros root locus, Fig. 5, we can see that it have six zeros and seven poles and modifying ω_c, only a real pole with th same ω_c value but negative, change position. A complex conjugate zero is crossing the imaginary axis illustrated in Fig. 5. As the system has zeros in the right-half side s-plane, it is a nonminimal phase system and the best way to study it is through the Nyquist diagram approach. We notice that when the real pole becomes closer to the origin the complex conjugate zero travel to the right, reducing its amplitude. Moreover, there are a fixed pair of conjugates dominant poles that when the real pole is approaching the origin, and the zeros travelling to the right, the ratio of the real part of the CL poles and the residues magnitudes are less than 5 then the resonant peak becomes smaller, and the system is well damped.[13]

Fig. 6 represents the frequency response of the OLTF of (12) for three different cut-off frequencies. When ω_c is 2200 rad/s, the magnitude peak response is the lowest (4.1 dB), as there is a relation between the damping ratio and the resonant peak, we can assume that setting ω_c at this value the transient response of the CLTF and the whole system is the better.

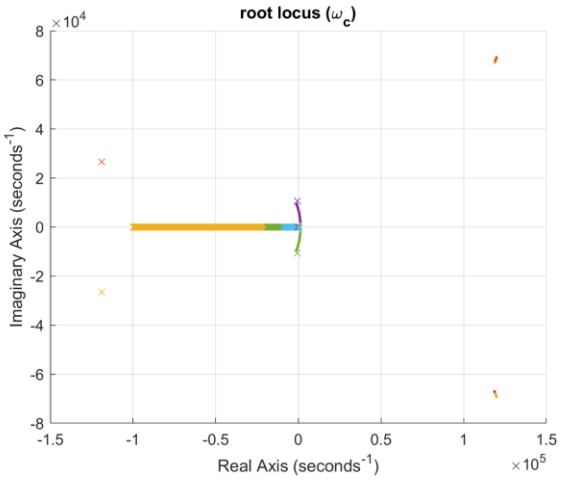

Fig. 5. Root locus plot modifying ω_c from 0 to 1x10^6 rad/s

Although, determine ω_c by studying the frequency response in OLTF of (12) and root locus diagram in CLTF it is insufficient because the behaviour of the actual system differed slightly. Nevertheless, a practical method has been applied through numerical methods: subtracting transfer function (12) from (13) to obtain the transient response for sinusoid waveforms inputs instead of constant steps and giving different values of ω_c from 0 to 1x10^6 rad/s. Then, finding the smallest maximum value of the input, we obtain the optimal ω_c. This method has been applied to a small signal digital model, including the sample time and the PWM saturation block, to approximate the real model better. It is important to say that the values of ω_c in each case are all around the same frequency, with slight differences due to the mathematical approximations of the models.

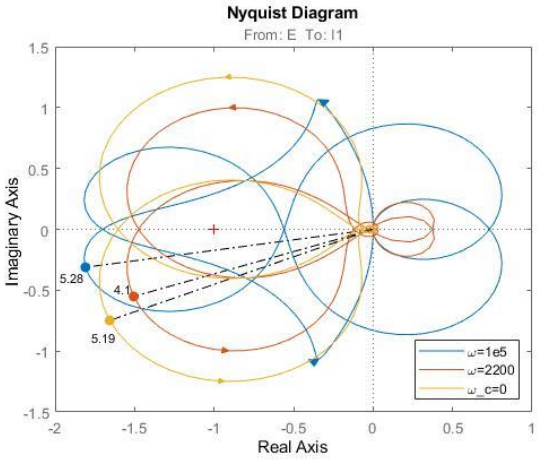

Fig. 6. OLTF Frequancy response

3 Results

The following tables shown the simulation results for the whole system modeled in transfer fnuctions with and without time delay with the real model whereas the graphs are the results of the real model

Table 3. I_1 peak (pu) considering the different configurations of FF and ω_c = 1x10^5 rad/s

FF topology	TF	TF_TD	Digital model	Real model
Static	N/A	N/A	1.716	1.899
Dynamic U_g (no derivative terms)	1.23	N/A	1.322	1.354
Dynamic HPF as a differentiator	1.115	1.149	1.196	1.255
hybrid	N/A	N/A	1.306	1.354

Table 4. I_1 peak (pu) considering the FF as a compensator for different ω_c values

ω_c(rad/s)	TF	TF_TD	Digital model	Real model
1x10^5	1.106	1.139	1.218	1.255
2400	1.072	1.088	1.092	1.104
2200	1.067	1.081	1.099	1.095
1800	1.056	1.069	1.122	1.112

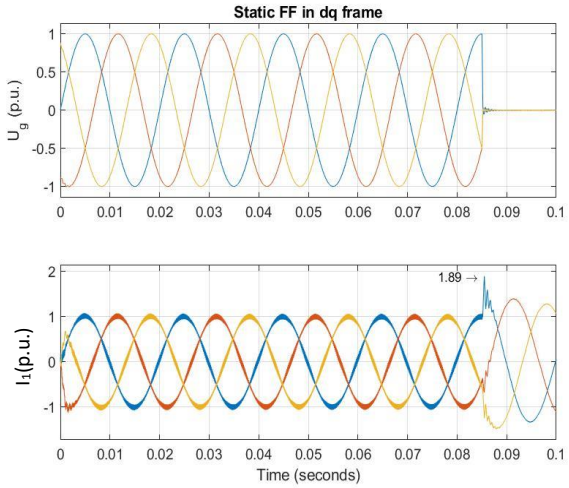

Fig. 7. First inductor current peak when static FF

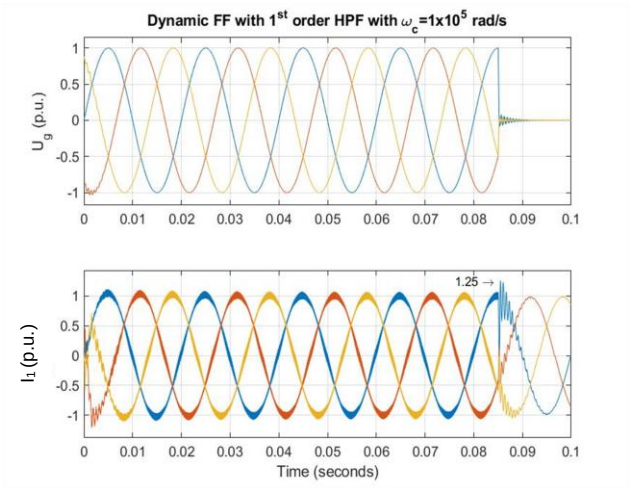

Fig. 8. First inductor current peak when FF with derivative term

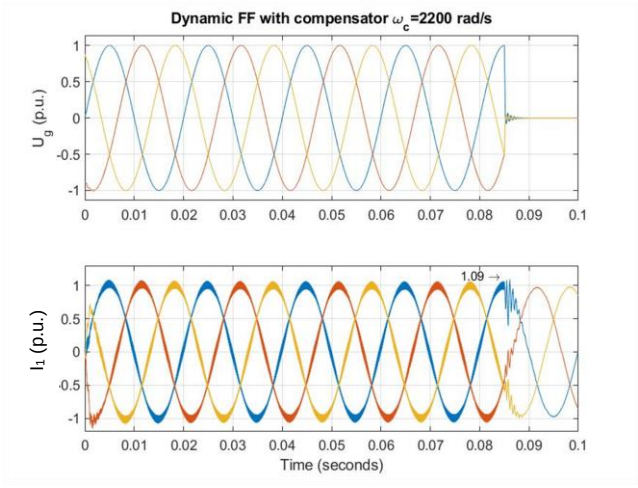

Fig. 9. First inductor current peak when FF as a compensator

4 Conclusion

According to the South African grid code, a detailed study has been conducted to determine the effect of the Voltage feedforward loop in the inductor current overshoot, with different implementation methods. The results show that the best Feedforward configuration to diminish the current transients in the inverter side is the dynamic Feedforward with the 1st order HPF approximated as a compensator, obtaining the lowest value from 1.89 p.u. Fig. 6 to 1.09 p.u. Fig. 8 Smaller than the maximum admissible 1.23 p.u. Therefore, we can conclude that a Feedforward loop is enough to tackle the current limit issue in the LVRT capability.

5 Acknowledgements

This work has been funded by the Royal Academy of Engineering Frontiers Follow-On Funding, as part of the Global Challenge Research Fund (GCRF) programme. Project Nr FF\1920\1\70 Socio-technical assessment for resilient electricity networks in rural Africa – STARENA.

6 References

[1] Power Futures Lab – Graduate School of Business South Africa. (October 2019). *Eskom: moving from crisis to a more sustainable future*.

[2] The Grid Code, N. G. E. S. O. *Limited Regulations*, 2020.

[3] *Grid Connection Code for Renewable Power Plants (RPPs) Connected to the Electricity Transmission System (TS) or the Distribution System (DS) in South Africa*, N. E. R. o. S. A. (NERSA), 2019.

[4] BDEW, "Guideline for generating plants' connection to and parallel operation with the medium-voltage network", June 2008

[5] N. Bottrell and T. C. Green, "Comparison of Current-Limiting Strategies During Fault Ride-Through of Inverters to Prevent Latch-Up and Wind-Up," *IEEE Trans. Power Electron.*, vol. 29, no. 7, pp. 3786-3797, 2014, doi: 10.1109/TPEL.2013.2279162.

[6] I. Sadeghkhani, M. E. H. Golshan, J. M. Guerrero, and A. Mehrizi-Sani, "A Current Limiting Strategy to Improve Fault Ride-Through of Inverter Interfaced Autonomous Microgrids," *IEEE Transactions on Smart Grid*, vol. 8, no. 5, pp. 2138-2148, 2017, doi: 10.1109/TSG.2016.2517201.

[7] Chou, S. F, Lee, C. T, Cheng, P. T, Blaabjerg, F." A Reactive Current Injection Technique for Renewable Energy Converters in Low Voltage Ride-Through Operations" 2011 Ieee Power and Energy Society General Meeting.

[8] Abusara, M., Sharkh, S., "Digital control of a three-phase grid connected inverter" 2011 International Journal of Power Electronics,Vol. 3 pp-299-319

[9] Abusara, M.,Sharkh, S. M, Zanchetta, P., "Control of grid-connected inverters using adaptive repetitive and proportional resonant schemes". 2015, Journal of Power Electronics, Vol.15, isssue 2 pp. 518-528

[10] J. Xu, Z. Zhang, S. Bian, M. Liu, S. Xie, "LCL-Filter Design to Suppress Transient Overshoots of Grid-Connected Inverters under Grid Voltage Fluctuations or Faults". 2019 IEEE Energy Conversion Congress and Exposition (ECCE). Pp. 2578-2582

[11] Abusara, Mohammad A., Sharkh, Suleiman M, Guerrero, Josep M." Improved droop control strategy for grid-connected inverters", 2015, Sustainable energy, grids and networks. pp. 10-1

[12] D. Pan, X. Ruan, X. Wang Direct Realisation of Digital Differentiators in Discrete Domain for Active Damping of LCL-Type Grid-Connected Inverter, 2018, IEEE Transactions on Power Electronics,Vol 33, pp-8461-8473

[13] Ogata, K. Modern Control Engineering, fourth Edition, 2002, Prentice-Hall.